ADVANCED MATERIALS

DOI: 10.1002/adma.200701766

An Efficient Route to Mesoporous Silica Films with Perpendicular Nanochannels**

By *Sivakumar Nagarajan*, *Mingqi Li*, *Rajaram A. Pai*, *Joan K. Bosworth*, *Peter Busch*, *Detlef-M. Smilgies*, *Christopher K. Ober*,* *Thomas P. Russell*,* and *James J. Watkins**

The fabrication of mesoporous silica films with well-defined morphologies[1] offers tremendous opportunity for device structures. In particular the generation of a mesoporous silica film with cylindrical nanochannels of prescribed diameters oriented normal to the substrate holds great promise for applications in catalysis,[2] bio-molecular separations, sensors,[3] photonics,[4] synthesis of aligned metallic nanowires[5–7] and carbon nanotubes[8–10] and for guest-host applications with electrically[11,12] and/or optically[13] active species. However fabricating well-defined, robust films by conventional evaporation-induced cooperative self-assembly approaches has proven to be extremely challenging.

[*] Prof. C. K. Ober, Dr. M. Li,[+] J. K. Bosworth, Dr. P. Busch[++]
Department of Materials Science and Engineering
Cornell University
Ithaca, NY, 14853 (USA)
E-mail: cober@ccmr.cornell.edu
Prof. T. P. Russell, Prof. J. J. Watkins, S. Nagarajan
Department of Polymer Science and Engineering
University of Massachusetts
Amherst, MA 01003 (USA)
E-mail: russell@mail.pse.umass.edu; watkins@polysci.umass.edu
Dr. R. A. Pai[+++]
Department of Chemical Engineering
University of Massachusetts
Amherst, MA 01003 (USA)
Dr. P. Busch, Dr. D.-M. Smilgies
Cornell High Energy Synchrotron Source (CHESS)
Cornell University
Ithaca NY, 14853 (USA)
[+] Present address: Rohm and Haas Electronic Materials, 455 Forest street, Marlborough, MA 01752, USA.
[++] Present address: JCNS, Research Centre Juelich GmbH, München, Lichtenbergstrasse 1, 85747 Garching, Germany.
[+++] Present address: Portland Technology Development Group, Intel Corporation, Hillsboro, OR 97124, USA.

[**] The authors thank the Materials Research Science and Engineering Center (MRSEC) (DMR-0213695) and the National Science Foundation Center for Hierachical Manufacturing (NSF-CHM) (CMMI-0531171) at the University of Massachusetts, Amherst & National Science Foundation Nanoscale Interdisciplinary Research Team Program (NSF-NIRT) (CTS-0304159) for financial support. This work was partially supported by the Cornell Center for Materials Research (CCMR), a Materials Research Science and Engineering Center of the National Science Foundation (DMR-0079992) and made use of the CCMR Electron Microscopy Facility. The Cornell High Energy Synchrotron Source (CHESS) is a national user facility supported by the National Science Foundation and the National Institutes of Health/National Institute of General Medical Sciences under award DMR-0225180. Supporting Information is available online from Wiley InterScience or from the authors.

The general approach to mesoporous materials is based on the discovery[14] that metal oxide precursors and structure-directing surfactants or amphiphilic block copolymers can self-assemble cooperatively to yield ordered composites from aqueous alcohol solutions via controlled solvent evaporation.[15,16] The organic surfactant can be removed to produce an inorganic mesoporous network. The size and shape of the pore are governed by the molecular mass and composition of the block copolymer, the nature of the precursor, solution acidity, temperature and concentration.[17] The ability to control pore size, morphology and orientation in these materials has been the subject of significant research[1,18,19] since their initial discovery.[14,20] While evaporation-induced cooperative self-assembly is a remarkably powerful approach, it has a number of limitations. One is poor control over orientational alignment of the cylindrical pores. Simultaneous structural evolution from cooperative block copolymer self-assembly and precursor condensation coupled with preferential affinity of one of the components of the sol solution for the interfaces (substrate/film or film/air) leads to a parallel orientation of the cylindrical pores with respect to the substrate. Magnetic fields[21] have been used as an external agent to align the cylindrical channels along the field direction. However, the direct preparation of mesoporous silica film with perpendicularly oriented cylindrical channels on conductive or non-conductive substrates without using any external agents has remained elusive. Recently it has been reported that porous anodic aluminum oxide membranes can be used as orientation inducing scaffolds to generate vertically aligned mesoporous silica channels within the pores of the membranes.[22,23] However, the preparation of the aluminum oxide scaffold is tedious and its use as a support produces a composite film containing only a small fraction of mesoporous silica channels. In this work, we demonstrate an efficient route to robust mesoporous silica films with nanochannels oriented normal to the substrate surface by a direct block copolymer template replication process.

Recently, we described a method to prepare robust mesoporous materials by a phase-selective silica deposition within a microphase separated block copolymer template dilated with supercritical carbon dioxide.[24] The use of supercritical fluid as a processing solvent enables facile transfer and reaction of precursors within the polymer film without disturbing the template order. The template can be removed to obtain a mesoporous inorganic replica. Unlike the conventional cooperative self assembly approach, our strategy for mesoporous met-

al oxide films decouples template self-assembly from metal oxide network formation. This enables an a priori definition of desired morphology in the template for direct replication in metal oxides.

There have been many successful efforts to orient the cylindrical domains of block copolymer films by controlling the interfacial interactions,[25,26] using external fields such as electric field,[6,27] shear,[28] graphoepitaxy,[29] crystallization,[30] temperature gradient[31] and chemically patterned substrates.[25] Solvent evaporation[32–34] and solvent annealing[35,36] can also be used as a non-invasive route to influence the orientation and lateral long range order of the cylindrical domains. Ober and coworkers, recently reported the synthesis of an amphiphilic block copolymer, poly(α-methyl styrene-*b*-hydroxy styrene) (PMS-PHOST).[37] It was found that the spin-coated films of PMS-PHOST exhibited a perpendicular orientation of the cylindrical microdomains of PMS over the entire thickness of the films. This block copolymer can be used as a template to generate mesoporous inorganic networks with vertical nanochannels by our direct replication approach.

Figure 1 depicts the overall scheme of this work. The organic template with the desired oriented morphology is prepared by spin-coating from a solution of amphiphilic block copolymer, comprised of ~ 70:30 ratios of hydrophilic and hydrophobic domains, and the acid catalyst. During solvent evaporation, the acid catalyst segregates selectively into the hydrophilic domain of the template. The template is then exposed to the silica precursor, TEOS, dissolved in humidified supercritical CO_2 ($scCO_2$). The presence of $scCO_2$, leads to moderate dilation of polymer films, which in turn facilitates rapid diffusion of precursor within the template.[38] Partitioning of acid catalyst ensures that hydrolysis and further condensation of precursor to metal oxide network occur only within the hydrophilic matrix and not in the hydrophobic cylinders or in the bulk fluid phase.[24] Moreover the alcohol formed as a by-product of alkoxide condensation is miscible with supercritical fluid phase and is rapidly extracted from the template, which drives the condensation towards completion and yields a nano-composite of the hydrophilic polymer domains interpenetrated with an inorganic network. After depressurization the organic component of the nano-composite can be removed by calcination to produce a mesoporous silica film with cylindrical pores oriented normal to the substrate surface.

The typical phase scanning force micrographs (PSFM) of 62.2K PMS-PHOST asymmetric block copolymer film obtained after spin coating onto a Si substrate and of the silica-infused nano-composite film obtained after phase-selective precursor condensation in supercritical CO_2 are shown in Figure 2. The phase signal in the PSFM images is sensitive to differences in the material properties of the two blocks such as adhesion, hardness and viscoelasticity.[39] The stronger the difference in the material properties of the two blocks, the higher the phase contrast in the image. In Figure 2a, the harder cylinders of hydrophobic PMS are oriented normal to the substrate in the relatively softer matrix of PHOST. The average lattice spacing distance of the cylindrical domains is ~ 37 nm with an average cylinder diameter of ~ 25 nm. It is worth mentioning that this particular template exhibits a modest lateral organization of cylindrical domains in the matrix (template lateral order) rather than a perfect hexagonal close packing. The weak lateral order could be attributed to the nonequilibrium state due to the fast evaporation of the solvent in the spin coating process and the high T_g of both the blocks. The inset in the figure shows the chemical structure of the block copolymer. Comparison of Figure 2a and b indicates that the template lateral order, domain dimensions and orientation remain essentially the same, while the phase contrast has become much higher between the matrix and the nanoscopic cylindrical micro domains. This is the result of the selective infusion of inorganic network in the hydrophilic matrix (and not in the hydrophobic cylindrical micro domains).

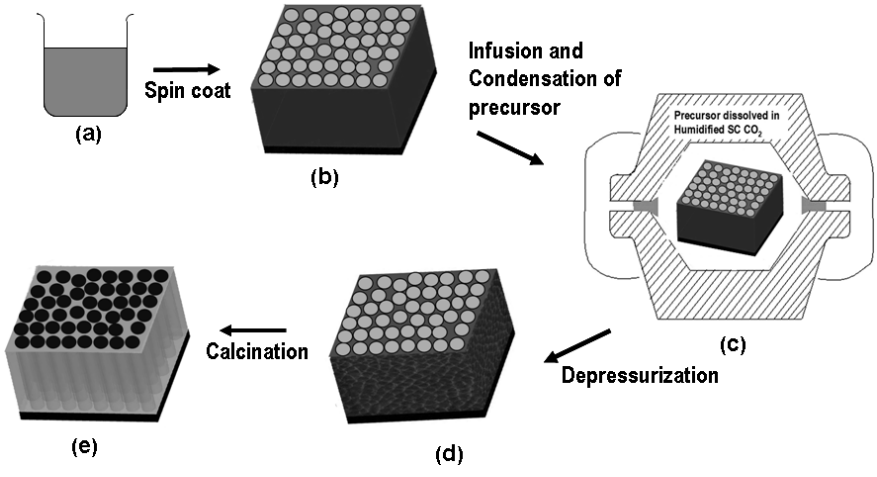

Figure 1. Schematic representation of synthesis of mesoporous silicate films with perpendicular nanochannels. Self assembled block copolymer film (b) with cylindrical domains oriented normal to the substrate is obtained by spin coating from the solution of block copolymer and acid catalyst (a). The film is dilated in humidified $scCO_2$ in the presence of TEOS, to form silica selectively in the hydrophilic domain (matrix) of the block copolymer template yielding the organic-inorganic nanocomposite film (d). The organic template is then removed to yield mesoporous silicate film with vertical nanochannels (e).

The silica-infused nano-composite film was then calcined at 400 °C for ~ 6 hours in air to remove the organic template and yield a complete inorganic network with perpendicular nanochannels. Top-down field emission scanning electron micrograph (FESEM) of the calcined mesoporous silica film (Fig. 3a) reveals the accessible porous channels oriented normal to the substrate in the matrix of silica. The diameter of the pores is essentially the same as that of the nanoscopic cylindrical do-

ADVANCED MATERIALS

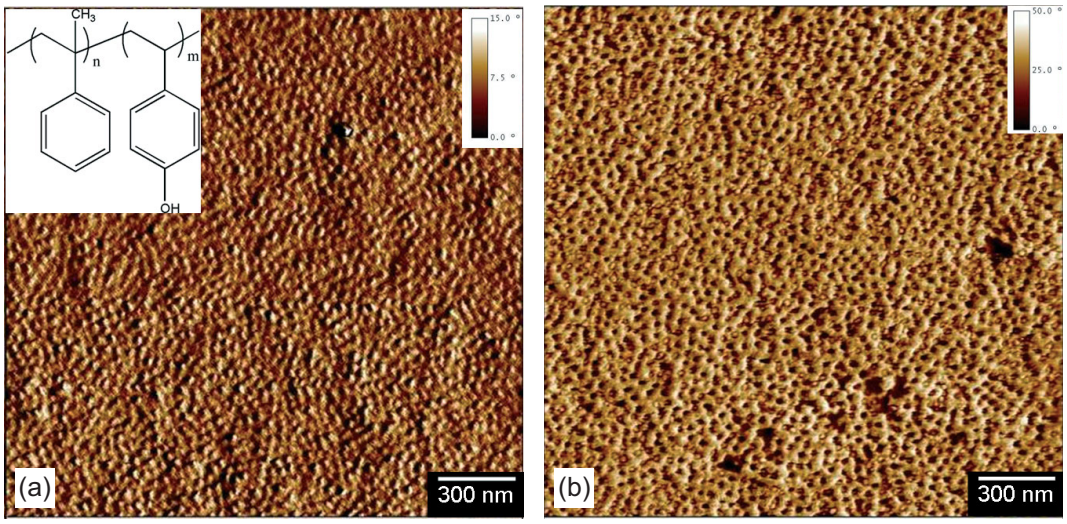

Figure 2. Phase scanning force micrograph of as-spun 62.2K PMS-PHOST film (a) and a corresponding 62.2K PMS-PHOST film infused with silica (b). Insets on the right of (a) and (b) show the corresponding SFM color scale. Inset on the left of (a) shows the chemical structure of PMS-PHOST.

mains of PMS in the block copolymer template. There is also a comparable degree of lateral order of domains/pores in the block copolymer template and in the mesoporous silica film. In order to probe the depth of the pores in the film, a very thin section of the film was imaged using transmission electron microscopy (TEM). The electron density contrast between silica and air is sufficient to easily determine the extent of penetration of the pores through the film. The TEM image in Figure 3b demonstrates the porous structures of the film which corresponds to the FESEM image (Fig. 3a), indicating that the pores probably span the entire thickness of the film. Dark areas in the image result from multiple layers of film where the electrons are attenuated. In order to obtain statistically averaged information on the internal structure of these films, grazing-incidence small angle X-ray scattering (GISAXS) was used. In GISAXS a highly collimated monochromatic X-ray beam impinges on the surface of the film at grazing angles.[40] The in-plane scattering provides information on the lateral correlation of the scatterers at the surface of the film or within the film.[41] By varying the incident angle below the critical angle of the film, depth-sensitive information can also be obtained.[42] The 2D-scattering profile of a 76 nm thick mesoporous silica film templated from the 62.2K PMS-PHOST is shown in Figure 4a. The scattering profile contains two prominent vertical streaks, indicative of porous channels oriented normal to the film surface.[35–37] The position of the scattering maxima with respect to the q_y axis, the scattering wave vector parallel to the surface of the film, corresponds to the lateral packing of the cylindrical pores. The q_y value of 0.01684 $Å^{-1}$, at scattering maxima, corresponds to the average d-spacing of 37.3 nm ($d_{spacing} = 2\pi/q_y$) in the XY plane of the film surface. The streaking of the scattering along q_z, the scattering wave vector normal to the surface of the film, corresponds to the truncation of the cylindrical channels at the surface of the film and at the substrate. It is worth mentioning that no other scattering intensity is seen in the profile, which strongly suggests that the film consists only of porous channels oriented normal to the surface. The absence of off-specular scattering (aside from the vertical streaks) essentially rules out the possibility of having 3-D or disordered structures within the film. The 1-D intensity profiles, plotted against q_y of the GISAXS data, collected for the same time in each case, of the as-spun 62.2K PMS-PHOST template (not shown), the silica-infused nanocomposite (not shown), and the calcined mesoporous silica film are plotted in the Figure 4d. The peak position in the as-spun film case corresponds to the d-spacing of 37.2 nm. The scattering profiles reveal that the as-infused and calcined films exhibit the same interdomain spacing as the "as-spun" template, indicating that the phase-selective silica infusion does not induce any change in the lateral dimensions of the structure. However, there is a significant intensity enhancement in the calcined film compared to the "as-infused" film and a slight increase in the scattering intensity in the "as-infused" film compared to the "as-spun" film. The intensity differences are expected, since the electron density contrast in the "as-spun" film is very low in comparison to that in the "as-infused" film. The electron density contrast is dramatically enhanced when the polymer is removed leaving only the silica matrix and cylindrical pores.

Silica infusion was carried out using three different molecular weight PMS-PHOST templates to demonstrate control over the pore size. Figure 4a–c shows the GISAXS patterns of the calcined mesoporous silica films, templated from 62.2K, 27.7K, and 22.9K PMS-PHOST, respectively. As the molecular weights of the templates decrease, the center-to-center (C–C) distance of nearest neighbor cylinders and the pore size decreases, i.e., the vertical streaks in GISAXS patterns move to higher q_y, which is also shown in the intensity profiles plotted in Figure 4e. The lower limit of the pore size that one can obtain using this process is dictated by the size of the do-

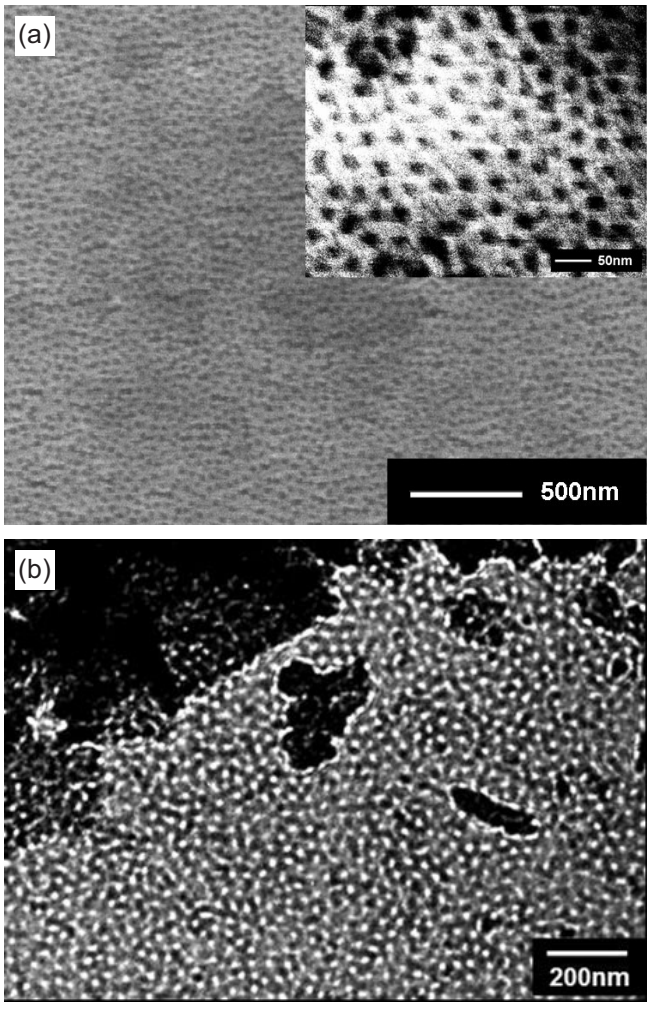

Figure 3. a) Field emission scanning electron micrograph of a calcined mesoporous silica film showing accessible pores oriented normal to the substrate. The inset displays a high magnification image of the same film. b) Transmission electron micrograph of a thin section of the mesoporous silica film.

mains in the block copolymer template. Cylinder-forming asymmetric block copolymers exhibit microphase separation when the product, χN, is greater than 13–14,[43,44] where χ is the interaction parameter between two blocks in the copolymer and N is the degree of polymerization. Smaller domain sizes can be achieved by choosing a system with high χ so that microphase separation occurs at relatively low degree of polymerization. As the χ is moderate in the system under study, we believe domain/pore sizes on the order of 10 nm can be achieved.

While, it was possible to determine the interference function, i.e., structure factor and the qualitative information about the shape of the scatterers from the GISAXS patterns, it was not possible to directly determine information about the size of the scatterers (form factor). GISAXS simulations done for similar geometrical conditions suggests that the oscillations, corresponding to the finite height of the cylindrical pores along q_z, can be completely smeared out if there is a slight distribution in the cylinder heights (See Supporting Information Fig. S1). In the measured GISAXS patterns, the initial oscillations in the vertical streak at low q_z are noticeable (Fig. 4a and b), but high q_z oscillations are smeared out. A distribution in the pore height can easily occur due to the roughness and thickness variations associated with thin films of a porous amorphous inorganic network as it is seen in the scanning electron micrograph of calcined mesoporous silica film (Fig. 3a).

In conclusion, we have shown that with the advances in controlling the orientation of block copolymer domains and a discrete two-step approach: i) template formation and ii) supercritical fluid assisted deposition, a straightforward preparation of mesoporous silica films with cylindrical pores oriented normal to the surface can be achieved. Such films are useful for the majority of applications that rely on vertical channels. One specific example is the fabrication of biochips with high-capacity DNA probe arrays.[45] Although PMS-PHOST block copolymer film serves as a suitable template to demonstrate an efficient route to mesoporous silica with perpendicular nanochannels, these templates lack long-range lateral order and therefore so does the final mesoporous silica films. Applications that rely on individually addressable arrays will require long range lateral order in both the template and the corresponding mesoporous silica film. Long range order in the block copolymer films has been achieved using solvent annealing and/or graphoepitaxy. The discrete two-step approach allows control over the domain size and orientation that can be used for device level definition of architectures. The photolithographic properties[37] of the block copolymer template will also enable the fabrication of directly patterned inorganic mesostructures with well defined structures at device length scales.

Experimental

Template Preparation: Asymmetric diblock copolymers of poly(hydroxy styrene) (PHOST) and poly(α-methyl styrene) (PMS), having molecular weights of 62,200 gm mol^{-1} (62.2K), 27,700 gm mol^{-1} (27.7K), and 22,900 gm mol^{-1} (22.9K) with PHOST volume fractions of 0.73, 0.72, and 0.65, respectively, were used as templates for synthesis of mesoporous silicate films. These diblock copolymers were synthesized by sequential anionic polymerization as described elsewhere [37]. The molecular weights and compositions were determined using SEC and NMR. Approximately 100 nm thick template films were prepared by spin coating solutions of block copolymer with catalytic amounts of p-toluenesulfonic acid (pTSA) in propylene glycol monomethyl ether acetate (PGMEA) onto undoped silicon substrates. The amount of pTSA was maintained at 3 wt % with respect to the mass of block copolymer in the solution. The spinning speed and time were maintained at 1500 rpm and 60 s, respectively. Solvent, PGMEA, pTSA, and the silicate precursor, tetraethylorthosilicate (TEOS), used in this study were purchased from Aldrich Inc.,

Phase-Selective Silica Infusion: Dilation of the block copolymer and condensation of TEOS within one phase of the template were performed in humidified supercritical carbon dioxide ($scCO_2$) at 60 °C and 125 bar in a high pressure reactor. The high-pressure reactor was built from two stainless steel blind hubs with a graphite-coated stain-

ADVANCED MATERIALS

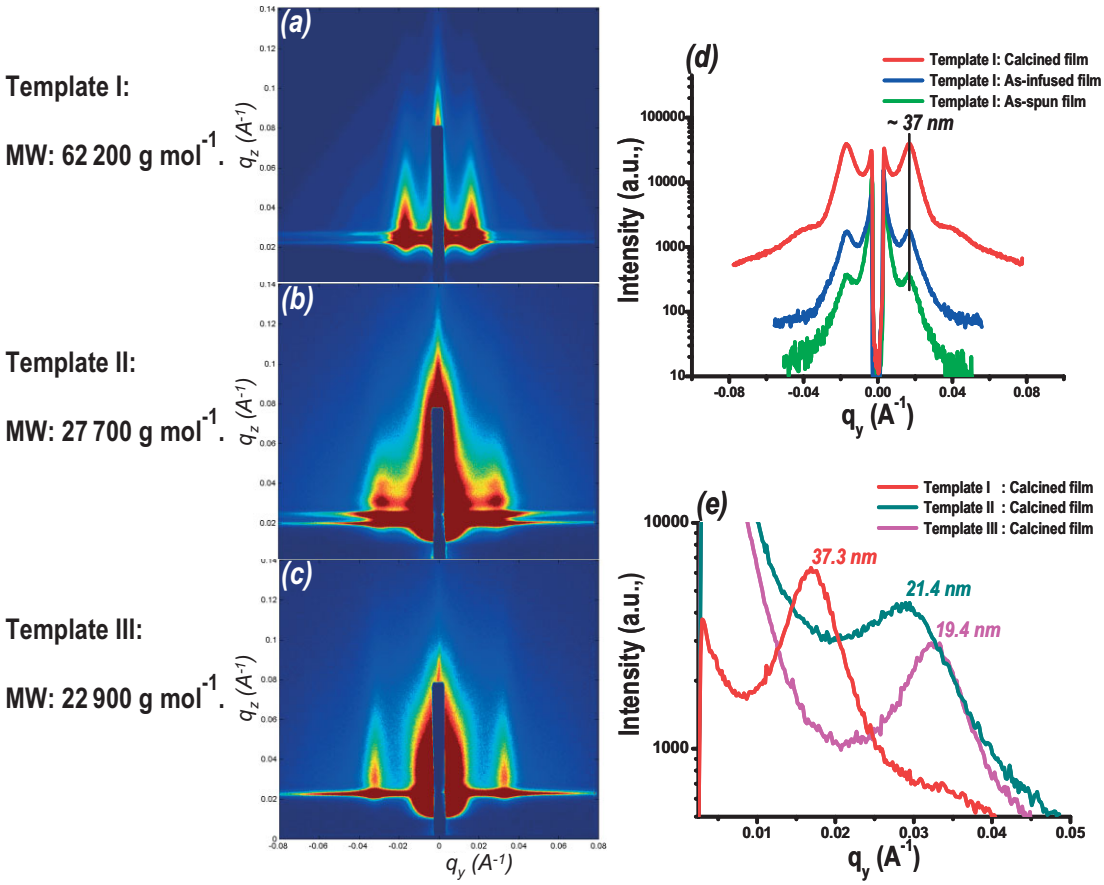

Figure 4. a–c) 2-D GISAXS scattering profiles of the calcined mesoporous silica film templated from 62.2K, 27.7K and 22.9K PMS-PHOST respectively. d) Intensity profiles plotted against lateral momentum transfer vector q_y of as-spun, silica-infused and calcined mesoporous silica film templated from 62.2K PMS-PHOST. As can be seen from the vertical line, serving as guide to the eyes, the cylinder spacing remains the same in each case. Note that the intensities for the silica-infused and the calcined samples are much larger than that in the as-spun sample due to increase in the electron-density contrast. e) Intensity profiles plotted against q_y for three different GISAXS patterns shown in (a–c). The center to center distances (C–C) are 19.4 nm, 21.4 nm, and 37.2 nm for the 22.9K, 27.7K, and 62.2K templates, respectively.

less steel seal ring. This reaction vessel has ~ 160ml of internal volume and machined ports for charging and discharging of CO_2 and for the measurements of temperature and pressure. A template film spun on ~ 1.25"×1.25" Si wafer piece was placed inside the reactor along with small amount of water (~ 0.5 g) and TEOS (1.0–5.0 μL). After sealing, the reactor was heated to 60 °C using external band heaters. CO_2 was then slowly injected into the reactor using a high-pressure syringe pump (ISCO, Inc. Model 500HP) until the desired pressure of ~ 125 bar was reached. Coleman-grade carbon dioxide (CO_2) was obtained from Merriam-Graves and used as received. The total pressurization and reaction time was maintained at 2 hours and then CO_2 was slowly released at the rate of ~ 0.3 bar min^{-1}. The organic template was removed from the nano-composite film by calcination at 400 °C for 6 hours in air using a heating rate of 1.67 °C min^{-1}.

Characterization of Organic Template and Mesoporous Silicate Films: The infusion of the silica and further removal of the organic template were qualitatively assessed by Fourier transform infrared spectrometer (Bio-Rad Excalibur Series FTS 3000). The surface morphologies of the films were imaged using a scanning force microscope (SFM, Digital Instruments Dimension 3000)and a scanning electron microscope (FESEM, JEOL 6320F instrument). Transmission electron microscopy was performed on calcined films using a JEOL 2000 CX microscope operating at 200 kV. The samples were prepared by scraping ~ 40 nm films off the substrate using a razor blade to make slurry of pieces of film in ethanol. A few drops of this slurry were dropped on the formvar resin-coated copper grid (Electron Microscopy Sciences) and dried prior to examination under microscope. Grazing incidence small angle X-ray scattering experiments were performed at D1 station of the Cornell High Energy Synchrotron Source (CHESS). The wavelength of X-rays used was 1.55 Å and the angle of incidence was chosen to be above the critical angle of the film under study, to make sure that the collected scattered radiation is the representation of the entire film thickness. The scattered radiation was collected with a two-dimensional charge-coupled device (CCD) camera with image sizes of 1024 pixels by 1024 pixels. The thickness of the films were measured using spectroscopic ellipsometer (Sopra Inc., GES5) and profilometer (Dektak3) and they were verified using X-ray reflectivity scans collected as a part of the GISAXS line-up process.

Received: July 19, 2007
Revised: October 3, 2007
Published online: December 20, 2007

[1] Y. Y. Wu, G. S. Cheng, K. Katsov, S. W. Sides, J. F. Wang, J. Tang, G. H. Fredrickson, M. Moskovits, G. D. Stucky, *Nat. Mater.* **2004**, *3*, 816.
[2] A. Sayari, *Chem. Mater.* **1996**, *8*, 1840.

[3] G. Wirnsberger, B. J. Scott, G. D. Stucky, *Chem. Commun.* **2001**, 119.
[4] M. Bockstaller, R. Kolb, E. L. Thomas, *Adv. Mater.* **2001**, *13*, 1783.
[5] Z. T. Zhang, S. Dai, D. A. Blom, J. Shen, *Chem. Mater.* **2002**, *14*, 965.
[6] T. Thurn-Albrecht, J. Schotter, C. A. Kastle, N. Emley, T. Shibauchi, L. Krusin-Elbaum, K. Guarini, C. T. Black, M. T. Tuominen, T. P. Russell, *Science* **2000**, *290*, 2126.
[7] D. Erts, B. Polyakov, E. Saks, H. Olin, L. Ryen, K. Ziegler, J. D. Holmes, in *Functional Nanomaterials for Optoelectronics and Other Applications*, Vol. 99/100, Trans Tech Publications, Zurich **2003**, p. 109.
[8] G. S. Duesberg, A. P. Graham, M. Liebau, R. Seidel, E. Unger, F. Kreupl, W. Hoenlein, *Nano Lett.* **2003**, *3*, 257.
[9] L. Huang, S. J. Wind, S. P. O'Brien, *Nano Lett.* **2003**, *3*, 299.
[10] Y. Murakami, S. Yamakita, T. Okubo, S. Maruyama, *Chem. Phys. Lett.* **2003**, *375*, 393.
[11] T. Q. Nguyen, J. J. Wu, V. Doan, B. J. Schwartz, S. H. Tolbert, *Science* **2000**, *288*, 652.
[12] W. J. Doherty, N. R. Armstrong, S. S. Saavedra, *Chem. Mater.* **2005**, *17*, 3652.
[13] A. Okabe, T. Fukushima, K. Ariga, T. Aida, *Angew. Chem. Int. Ed.* **2002**, *41*, 3414.
[14] C. T. Kresge, M. E. Leonowicz, W. J. Roth, J. C. Vartuli, J. S. Beck, *Nature* **1992**, *359*, 710.
[15] S. Forster, M. Antonietti, *Adv. Mater.* **1998**, *10*, 195.
[16] P. D. Yang, D. Y. Zhao, D. I. Margolese, B. F. Chmelka, G. D. Stucky, *Nature* **1998**, *396*, 152.
[17] M. Imperor-Clerc, P. Davidson, A. Davidson, *J. Am. Chem. Soc.* **2000**, *122*, 11925.
[18] C. J. Brinker, Y. F. Lu, A. Sellinger, H. Y. Fan, *Adv. Mater.* **1999**, *11*, 579.
[19] A. Gibaud, D. Grosso, B. Smarsly, A. Baptiste, J. F. Bardeau, F. Babonneau, D. A. Doshi, Z. Chen, C. J. Brinker, C. Sanchez, *J. Phys. Chem. B* **2003**, *107*, 6114.
[20] J. S. Beck, J. C. Vartuli, W. J. Roth, M. E. Leonowicz, C. T. Kresge, K. D. Schmitt, C. T. W. Chu, D. H. Olson, E. W. Sheppard, S. B. McCullen, J. B. Higgins, J. L. Schlenker, *J. Am. Chem. Soc.* **1992**, *114*, 10834.
[21] S. H. Tolbert, A. Firouzi, G. D. Stucky, B. F. Chmelka, *Science* **1997**, *278*, 264.
[22] A. Yamaguchi, F. Uejo, T. Yoda, T. Uchida, Y. Tanamura, T. Yamashita, N. Teramae, *Nat. Mater.* **2004**, *3*, 337.
[23] Q. Y. Lu, F. Gao, S. Komarneni, T. E. Mallouk, *J. Am. Chem. Soc.* **2004**, *126*, 8650.
[24] R. A. Pai, R. Humayun, M. T. Schulberg, A. Sengupta, J. N. Sun, J. J. Watkins, *Science* **2004**, *303*, 507.
[25] E. Huang, L. Rockford, T. P. Russell, C. J. Hawker, *Nature* **1998**, *395*, 757.
[26] P. Mansky, Y. Liu, E. Huang, T. P. Russell, C. Hawker, *Science* **1997**, *275*, 1458.
[27] T. L. Morkved, M. Lu, A. M. Urbas, E. E. Ehrichs, H. M. Jaeger, P. Mansky, T. P. Russell, *Science* **1996**, *273*, 931.
[28] R. J. Albalak, E. L. Thomas, M. S. Capel, *Polymer* **1997**, *38*, 3819.
[29] R. A. Segalman, H. Yokoyama, E. J. Kramer, *Adv. Mater.* **2001**, *13*, 1152.
[30] C. De Rosa, C. Park, E. L. Thomas, B. Lotz, *Nature* **2000**, *405*, 433.
[31] J. Bodycomb, Y. Funaki, K. Kimishima, T. Hashimoto, *Macromolecules* **1999**, *32*, 2075.
[32] G. Kim, M. Libera, *Macromolecules* **1998**, *31*, 2569.
[33] G. Kim, M. Libera, *Macromolecules* **1998**, *31*, 2670.
[34] Z. Q. Lin, D. H. Kim, X. D. Wu, L. Boosahda, D. Stone, L. LaRose, T. P. Russell, *Adv. Mater.* **2002**, *14*, 1373.
[35] S. H. Kim, M. J. Misner, T. Xu, M. Kimura, T. P. Russell, *Adv. Mater.* **2004**, *16*, 226.
[36] S. H. Kim, M. J. Misner, T. P. Russell, *Adv. Mater.* **2004**, *16*, 2119.
[37] M. Q. Li, K. Douki, K. Goto, X. F. Li, C. Coenjarts, D. M. Smilgies, C. K. Ober, *Chem. Mater.* **2004**, *16*, 3800.
[38] R. R. Gupta, V. S. RamachandraRao, J. J. Watkins, *Macromolecules* **2003**, *36*, 1295.
[39] R. Garcia, A. San Paulo, *Phys. Rev. B* **1999**, *60*, 4961.
[40] J. R. Levine, L. B. Cohen, Y. W. Chung, P. Georgopoulos, *J. Appl. Crystallogr.* **1989**, *22*, 528.
[41] D. M. Smilgies, P. Busch, D. Posselt, C. M. Papadakis, *Synchrotron Radiat. News* **2002**, *15*, 35.
[42] B. J. Factor, T. P. Russell, M. F. Toney, *Phys. Rev. Lett.* **1991**, *66*, 1181.
[43] L. Leibler, *Macromolecules* **1980**, *13*, 1602.
[44] J. D. Vavasour, M. D. Whitmore, *Macromolecules* **1992**, *25*, 5477.
[45] M. Glazer, J. Fidanza, G. McGall, C. Frank, *Chem. Mater.* **2001**, *13*, 4773.

